Semnan University

Progress in Physics of Applied Materials

journal homepage: https://ppam.semnan.ac.ir/

Improving the efficiency of dye sensitized solar cell with Titanium doping of Tin oxide photoanode

S. Pazouki, N. Memarian*

Faculty of Physics, Semnan University, P.O. Box: 35195-363, Semnan, Iran.

ARTICLE INFO

Article history:
Received: 7 September 2022
Revised: 4 October 2022
Accepted: 11 October 2022

Keywords:
Dye sensitized solar cell
Nanoparticles
Tin oxide
Titanium doping

ABSTRACT

In this article, tin oxide nanoparticles were prepared by hydrothermal method and then deposited on fluorine doped tin oxide (FTO) glass by Dr. Blade method and dye sensitized solar cell (DSSC) was fabricated with tin oxide photoanode. To improve cell efficiency, the prepared photoanode was doped with titanium and the effect of Ti doping on physical properties and performance of DSSCs were investigated. The physical properties of the synthesized nanostructures were investigated by XRD, SEM, BET, and DRS analyses. Finally, DSSC solar cells were constructed from prepared photoanodes and current-voltage analysis was performed. The results showed that Ti doping affects the adsorption-desorption isotherm of the sample and increases the specific surface area significantly. Thus, specific surface area has increased from 36.23 m^2/g for the SnO_2 sample to 508.13 m^2/g for the Ti doped sample. The results showed that the DSSC made with doped photoanode showed much better performance and titanium doping increased both the short circuit current and open circuit voltage. The titanium doped sample showed an increase in efficiency of about 2 times compared to the pure SnO_2 photoanode.

1. Introduction

Despite many developments in science and technology, the majority of the world's energy is still supplied through fossil and non-renewable fuels, which leads to environmental pollution and, in particular, an increase in carbon in the environment [1]. On the other hand, the use of renewable energy sources leads to the creation of a clean and healthy environment [2,3]. There are various renewable energy sources such as wind energy, solar energy, and hydro energy. Solar energy is one of the suitable renewable energy sources due to its availability, simple principles, easy and low-cost construction of conversion devices. By using a solar cell (photovoltaic cell), the sun's energy can be directly converted into electricity [4].

Today, most of the research in solar cell field is focused on the third generation solar cells, which are based on nanotechnology. Among different types of nanostructured solar cells, dye sensitized solar cells (DSSCs) are very attractive due to low cost of production, variety of colors and shapes, eco-friendliness, flexibility, and light weight [5]. One of the most important components of a DSSC is its photoanode (or working electrode), which usually a semiconductor with a wide gap is used as a photoanode. Titanium oxide [6], zinc oxide [7], niobium oxide [8], and tin oxide [9] are among the most common semiconductors used as photoanodes in DSSCs. Also, using different structures such as hybrid nanostructures, doping, core-shell, and decorating structures are the strategies to increase DSSCs efficiency [10].

An appropriate photoanode should have a large specific surface area for better absorption of the dye as well as higher separation and transferring the photoelectrons. On the other hand, its band structure should be such that it prevents the recombination of photoelectrons on the surface of the dye and their reverse movement towards the electrolyte [11].

In most DSSCs, TiO_2 is used as the photoanode. However, some other semiconductors, such as ZnO or SnO_2 have better physical properties (i.e., electrical conductivity, optical response, higher electron lifetime, …) but they have been used less than TiO_2. The aim of this work is to improve the DSSC performance with SnO_2 photoanode. In this article, tin dioxide nanoparticles were prepared by hydrothermal method, then coated on FTO (fluorine doped

* Corresponding author. Tel.: +98-912-2312970
E-mail address: n.memarian@semnan.ac.ir

DOI: 10.22075/PPAM.2022.28325.1034

tin oxide) substrate by Dr. Blade method. In order to improve the efficiency of the cells, the photoanode was doped with titanium ions. The main advantage of this work method and our synthesis process is that SnO_2 nanospheres have been synthesized from Na_2SnO_3 precursor (different from normal chloride precursors) and without using any surfactant and/or template, to reduce the synthesis cost.

2. Experimental

First, by using 0.4668 g of precursor ($Na_2SnO_3.3H_2O$, Merck), 70cc solution of deionized water and ethanol (with a volume ratio of 52.5/) was prepared. Then, the resulting milky solution was poured into the Teflon-lined autoclave and kept in the oven for 20 hours at a temperature of 150°C to complete the hydrothermal process. Then the precipitate was washed 4 times with distilled water and ethanol and centrifuged. After that it was dried in the oven at 90°C for 70 minutes and then, it was calcined at 500°C for 1 hour.

In order to fabricate the photoanode layer on the FTO substrate, a paste was prepared from the prepared powder (0.6 g) by using deionized water (0.5 ml), pure ethanol (2.5 ml), alpha-terpineol (0.5 ml) and ethyl cellulose (0.25 g) [12, 13]. The paste was ultrasonicated for half an hour and then placed on a magnetic stirrer for 24 hours. Then photoanodes were prepared by Dr. Blade method and tin oxide photoanode was prepared.

In order to dope the photoanodes with titanium, they are immersed in a solution containing 1.3 % (by volume) of titanium butoxide (TBT) for 45 minutes at a temperature of 70°C and then placed in an oven at a temperature of 70°C for 1 hour to stabilize and dry. The pure tin oxide sample and the sample doped with Ti were named SnO2 and STO, respectively. The photoanodes were immersed in N719 dye (0.5 mM) for 24 hours. Next, by using platinum coated FTO (as cathode) and Surlyn polymer, the cells were sealed and iodide/triiodide electrolyte was injected and the I-V analysis was done under solar simulator.

The crystalline structure and the microstructural morphology of the samples were studied by X-ray diffraction analysis (XRD) analysis (Advance Bruker D-8) and Field-emission scanning electron microscopy, FESEM (MIRA3TESCAN-XMU), respectively. The Brunauer–Emmett–Teller (BET) method was carried out (Belsorp mini, Japan) at 77 K with N_2 gas to find out the specific surface area of the samples. Pore size distribution curves were also estimated from the desorption branch of the isotherms using the Barrett–Joyner–Halenda (BJH) algorithm. Diffuse reflectance spectra (DRS) of the samples were measured with an Avantes AvaSpec 3648 spectrophotometer. The I-V curve of fabricated DSSCs was recorded under calibrated solar simulator (Sharif Solar) with a potentiostat device.

3. Results and discussion

The crystalline structure of the samples was studied by XRD analysis. Fig. 1 shows the XRD patterns of the samples. Both samples showed diffraction peaks at the angles of 26.4, 33.8, 38.1, and 51.9, which correspond to the JCPDS card number 072-1147 and corresponding to the crystal planes of (110), (101), (111), and (211), respectively. Analysis with Xpert software showed that the samples were pure tin dioxide with tetragonal crystalline structure and P24/mnm space group. Titanium impurity did not cause any additional peaks in the XRD spectrum and it seems that it had no effect on the crystal structure of the sample and titanium atoms replaced tin atoms in the SnO_2 structure.

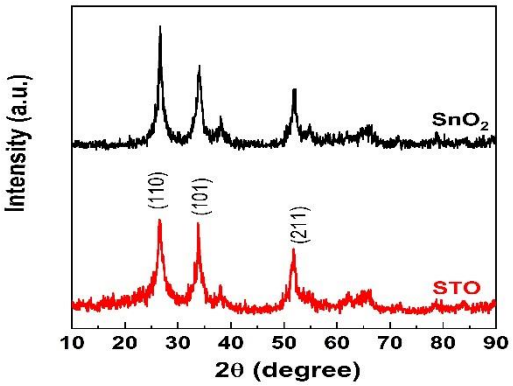

Fig. 1. XRD patterns of the samples.

The crystallite size was calculated using the Debye-Scherer method [14-17]:

$$D = \frac{k\lambda}{\beta \cos\theta} \quad (1)$$

Where, k is a constant (0.9), λ is the wavelength of X-ray radiation source (1.54 Å), β is the width of the peak at half maximum height (FWHM) and θ is the Bragg angle. The crystallite sizes were found 17.8 nm for the SnO_2 sample and 6.6 nm for the STO sample. It seems that by Ti doping the crystallite size reduced, which could be due to the substitution of Ti atoms in the Sn sites in the lattice.

In order to study the microstructure and morphology of the samples, FESEM analysis was conducted. Fig. 2 shows FESEM images of SnO_2 (Fig.2a) and STO (Fig.2b) samples. As can be seen in Figure 2(a), the pure tin oxide sample is composed of nanospheres which have an almost uniform size distribution. But with titanium doping, the morphology has changed and the uniformity in the size of the nanoparticles has been lost. Some of the nanospheres have merged and larger particles have been formed. Also, agglomeration of nanoparticles can be seen. This change in the microstructure and morphology of the sample can affect the effective surface area and other characteristics of the synthesized structure, which are discussed below.

By using BET analysis very interesting information such as the specific surface area, the average size of the pores and the total volume of the pores in the sample is obtained. Fig. 3(a) shows the adsorption-desorption isotherm of the samples and Figure 3(b) shows the size distribution of the holes. Both samples have a hysteresis loop in the absorption branch. Since the desorption branch is connected to the adsorption branch at low relative pressures, both samples tend towards microporous structure. According to the IUPAC classification [18], the type of isotherm for the SnO_2 sample is pseudo-IV isotherm, and for the STO sample, the isotherm type is changed and more consistent with the

type II isotherm. Both samples have H4 type hysteresis. The results of BET analysis are given in Table 1. By calculating the specific surface area of the samples, it can be seen that the specific surface of the samples increased with titanium doping significantly. Thus specific surface area has increased from 36.23 m^2/g for the SnO_2 sample to 508.13 m^2/g for the STO sample. This remarkable increase in the specific surface area of the doped sample could be due to the second thermal treatment and rearrangement of atoms in the crystal structure of the sample. In addition, the total pore volume has increased from 0.0945 cm^3/g to 0.2184 cm^3/g, which confirms the increase in porosity in the STO sample. Furthermore, the average pore size has decreased from 10.486 to 1.719 nm for the doped sample. This increase in the specific surface area and the porosity of photoanode can be the origin of increase in dye absorption on the surface of the photoanode, and as a result, the increase in the photoelectrons generation in the solar cell.

Fig. 4(a) shows the Diffuse Reflectance spectra of the samples. It is clear that both samples have a high reflectance in the visible and NIR region. By using the DRS spectrum, the absorption coefficient of the samples is calculated using the Kubelka–Munk equation [19,20].

$$F(R)=\frac{\alpha}{S}=\frac{(1-R)^2}{2R} \quad (2)$$

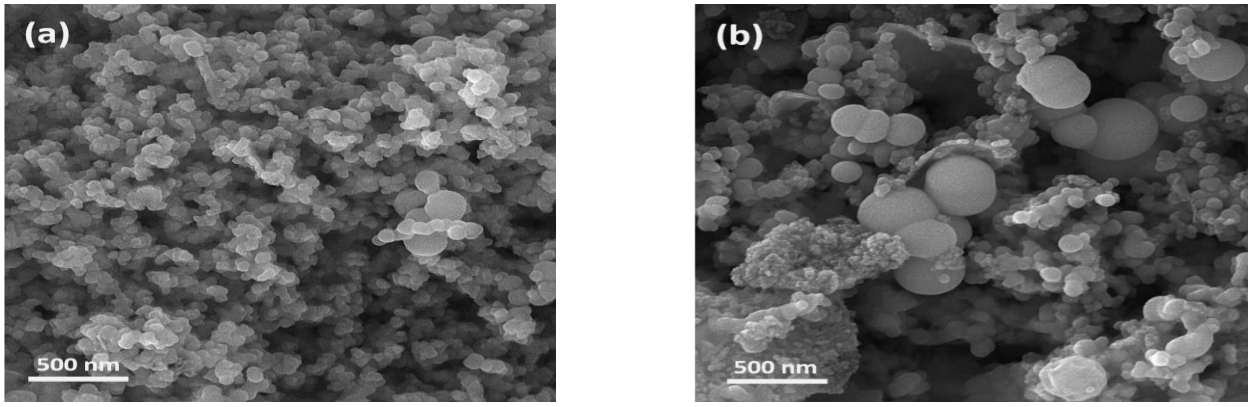

Fig. 2. FESEM images of (a) SnO_2 and (b) STO samples.

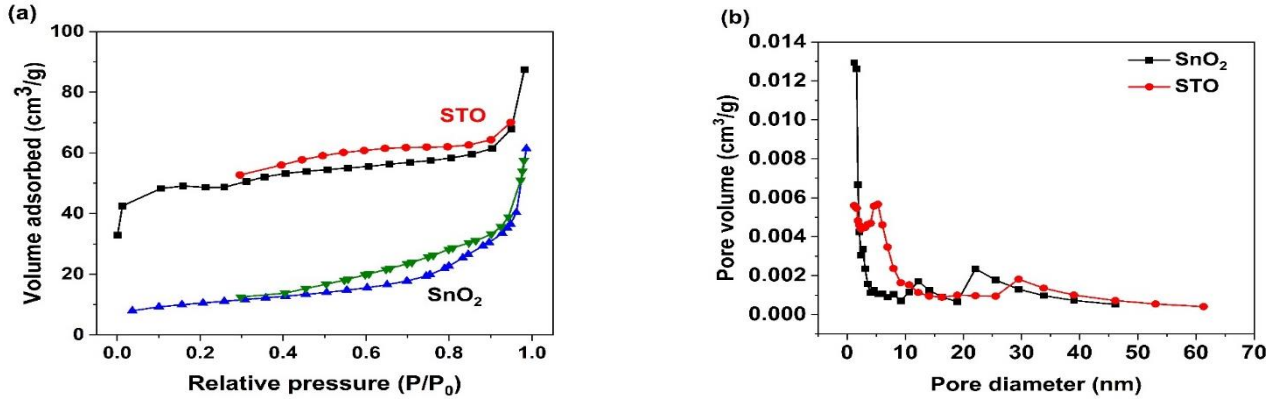

Fig. 3. (a) absorption-desorption isotherms and (b) Pore size distribution for tin oxide and titanium doped tin oxide nanopowders.

Table 1. BET analysis results.

sample	Specific surface area (m^2/g)	Total pore volume (cm^3/g)	Average pore size (nm)
SnO_2	36.23	0.094	10.49
STO	508.1	0.218	1.719

where F(R), α, S, and R are Kubelka–Munk function, absorption coefficient, scattering factor, and reflectance of the sample, respectively. Since S is a constant and does not change with wavelength, it can be ignored and F(R) is assumed to be directly proportional to the absorption coefficient. Then, the band gap of sample is calculated by using Tauc equation (eq.3) [21]:

$$F(R)\cdot h\upsilon = A\left(h\upsilon - E_g\right)^n \quad (3)$$

Where A is constant and power n depends on the type of transition. For direct allowed transitions, n=1/2 and n=2 for indirect transitions. By extrapolating the linear part of plot to the energy axis, the band gap energy value is obtained, which is 3.37 and 3.41 eV for SnO_2 and STO samples, respectively.

The calculated band gap here is lower than that of bulk SnO_2 gap (i.e. 3.6 eV.). This band gap shrinkage is reported in the literature [20, 22] and might be due to the ultrafine

crystallite size of the samples and so the increase of unit cell parameters [23].

Finally, current-voltage analysis was taken from the fabricated DSSCs. Figure 5 shows the I-V curve for the assembled solar cells. The obtained results are shown in Table 2. The fill factor (FF) and efficiency (η) of the fabricated DSSCs are calculated by the following equations respectively[24]:

$$FF = \frac{V_{\max} J_{\max}}{V_{OC} J_{SC}} \quad (4)$$

$$\eta = \frac{V_{OC} J_{SC} FF}{P_{in}} \quad (5)$$

where, Voc is open circuit voltage, Jsc is short circuit current density, Vmax and Jmax are the voltage and current of maximum power point respectively, and P_{in} is the incident power of light [24]. As it can be clearly seen, Ti doping has increased both the short circuit current and the open circuit voltage in the solar cell. This could be attributed to the increase of specific surface area and higher dye loading on the surface of photoanode, which directly increase the photocurrent in DSSCs.

Table 2. functional parameters of fabricated DSSCs.

sample	Jsc (mA/cm^2)	Voc (V)	FF	Efficency (%)
SnO_2	2.74	0.40	0.33	0.36
STO	3.62	0.53	0.37	0.68

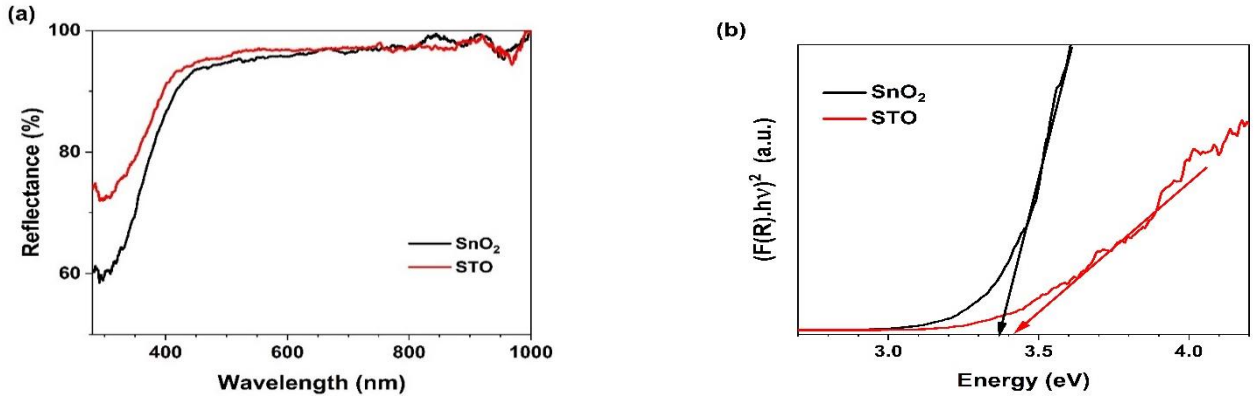

Fig. 4. (a) DRS spectra and (b) Tauc plots of the samples.

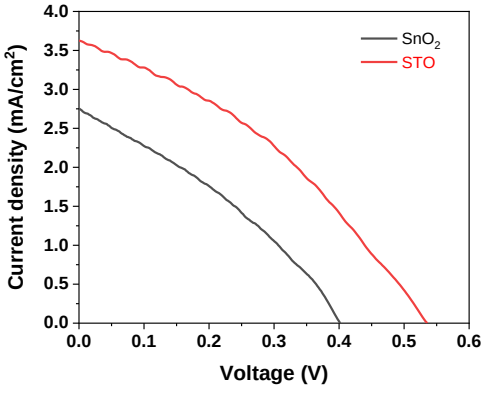

Fig. 5. J-V curves of DSSCs prepared with SnO_2 and STO photoanodes.

4. Conclusion

In this article, spherical nanoparticles of tin oxide and tin oxide doped with titanium were synthesized. Then these nanostructures were used as photoanode in dye solar cell. The XRD analysis results showed that tin oxide nanostructures were synthesized without any impurity or secondary phase. BET analysis of the samples confirmed a significant increase in the specific surface area of photoanode by Ti doping. I-V analysis revealed increasing in both Jsc and Voc. The efficiency increased from 0.36% to 0.68%.

References

[1] G. Richhariya, B. Meikap, A. Kumar. "Review on fabrication methodologies and its impacts on performance of dye-sensitized solar cells." Environmental Science and Pollution Research (2022) 1-19.

[2] A. Sharma, J. Srivastava, A. Kumar. "A comprehensive overview of renewable energy status in India." Environmental Sustainability (2015) 91-105.

[3] A. Awasthi, A. K. Shukla, M. Manohar SR, Chandrakant Dondariya, K. N. Shukla, D. Porwal, G. Richhariya. "Review on sun tracking technology in solar PV system." Energy Reports 6 (2020) 392-405.

[4] J.A. Castillo-Robles, E. Rocha-Rangel, J.A. Ramírez-de-León, F.C. Caballero-Rico, E.N. Armendáriz-Mireles, "Advances on Dye-Sensitized Solar Cells (DSSCs) Nanostructures and Natural Colorants: A Review." Journal of Composites Science 5 (2021) 288.

[5] X. Wang, B. Zhao, W. Kan, Y. Xie, K. Pan. "Review on Low-Cost Counter Electrode Materials for Dye-Sensitized Solar Cells: Effective Strategy to Improve Photovoltaic

Performance." Advanced Materials Interfaces 9 (2022) 2101229.
[6] A. Omar, M.S. Ali, N. Abd Rahim" Electron transport properties analysis of titanium dioxide dye-sensitized solar cells (TiO_2-DSSCs) based natural dyes using electrochemical impedance spectroscopy concept: A review." Solar Energy 207 (2020) 1088-1121.
[7] M. Salem, N. Memarian. "Fabrication and characterization of dye-sensitized solar cells based on nanostructured ZnO photoanodes." Journal of Coupled Systems and Multiscale Dynamics 5 (2017) 27-32.
[8] M. Memari, N. Memarian. "Designed structure of bilayer TiO_2–Nb_2O_5 photoanode for increasing the performance of dye-sensitized solar cells." Journal of Materials Science: Materials in Electronics 31 (2020) 2298-2307.
[9] A. Zatirostami, "SnO_2-based DSSC with SnSe counter electrode prepared by sputtering and selenization of Sn: Effect of selenization temperature." Materials Science in Semiconductor Processing 135 (2021) 106044.
[10] H.A. Shittu, I. T. Bello, M. A. Kareem, M. K. Awodele, Y. K. Sanusi, O. Adedokun. "Recent developments on the photoanodes employed in dye-sensitized solar cell." In IOP Conference Series: Materials Science and Engineering, vol. 805, no. 1, p. 012019. IOP Publishing, 2020.
[11] X. Miao, K. Pan, Y. Liao, W. Zhou, Q. Pan, G. Tian, G. Wang. "Controlled synthesis of mesoporous anatase TiO_2 microspheres as a scattering layer to enhance the photoelectrical conversion efficiency." Journal of Materials Chemistry A 1 (2013) 9853-9861.
[12] G. Selopal, N. Memarian, R. Milan, I. Concina, G. Sberveglieri, A. Vomiero. "Effect of blocking layer to boost photoconversion efficiency in ZnO dye-sensitized solar cells." ACS Applied Materials & Interfaces 6 (2014) 11236-11244.
[13] S. Ito, P. Chen, P. Comte, M.K. Nazeeruddin, P.Liska, P. Péchy, M. Grätzel. "Fabrication of screen-printing pastes from TiO_2 powders for dye-sensitised solar cells." Progress in photovoltaics: research and applications 15 (2007) 603-612.
[14] T. Raoufi, M. H. Ehsani, D. Sanavi Khoshnoud. "Critical behavior near the paramagnetic to ferromagnetic phase transition temperature in $La_{0.6}Sr_{0.4}MnO_3$ ceramic: a comparison between sol-gel and solid state process." Ceramics International 43 (2017) 5204-5215.
[15] E. Farahi, N. Memarian. "Surfactant-assisted synthesis of Ni_2P nanostructures: effect of surfactant concentration on photocatalytic activity." The European Physical Journal Plus 137 (2022) 463.
[16] N. Memarian, S. M. Rozati. "Effect of deposition conditions on physical properties of SnO_2 thin films prepared using the spray pyrolysis technique." Canadian Journal of Physics 90 (2012) 277-281.
[17] M. Rabizadeh, M.H. Ehsani. "Effect of heat treatment on optical, electrical and thermal properties of ZnO/Cu/ZnO thin films for energy-saving application." Ceramics International 48 (2022) 16108-16113.
[18] M. Kruk, M. Jaroniec. "Gas adsorption characterization of ordered organic– inorganic nanocomposite materials." Chemistry of materials, 13 (2001) 3169-3183.
[19] Z.H. Yamani, J. Iqbal, A. Qurashi, A.s Hakeem. "Rapid sonochemical synthesis of In_2O_3 nanoparticles their doping optical, electrical and hydrogen gas sensing properties." Journal of alloys and compounds 616 (2014) 76-80.
[20] S. Khajuee, N. Memarian. "Hydrothermal synthesis of ultrafine SnO_2 nanospheres: effect of reaction time on physical properties." The European Physical Journal Plus 136 (2021) 1-12.
[21] E. Farahi, N. Memarian. "Nanostructured nickel phosphide as an efficient photocatalyst: effect of phase on physical properties and dye degradation." Chemical Physics Letters 730 (2019) 478-484.
[22] B. Babu, J. Shim, K. Yoo. "Effects of annealing on bandgap and surface plasmon resonance enhancement in Au/SnO_2 quantum dots." Ceramics International 46 (2020) 17-22.
[23] N. Kamarulzaman, N. Aziz, M. Kasim, N. Chayed, R.Subban, N. Badar. "Anomalies in wide band gap SnO_2 nanostructures." Journal of Solid State Chemistry 277 (2019) 271-280.
[24] M. Jao, H.Liao, W. Su. "Achieving a high fill factor for organic solar cells." Journal of Materials Chemistry A 4 (2016) 5784-5801.